Research

Computer Simulation of Flow of Air and Methane Mixture in the Longwall – Return Crossing Zone

Marian Branny

Address: AGH University of Science and Technology, 30-059 Krakow, al. Mickiewicza30, Poland

Email: branny@agh.edu.pl

Published: 31 March 2007

This article has been published jointly by PJO and Archives of Mining Sciences (AMS), Transactions of Polish Academy of Sciences (Vol. 51, Issue 1) by permission of AMS.

E-Journal of Mining Engineering, 2007

This article is available from: http://www.petroleumjournalsonline.com/

Abstract

This paper investigates how the positions of jet fans, installed at the outlet from the longwall region, should affect the efficiency of methane rarefaction and removal from the area. The adequacy of the suggested solution is verified by numerical simulations supported by the programme FLUENT 6.1.

The flow region comprising two crossing headings (longwall end section with the return airway) is shown in Fig 1. Methane inflow from the rock strata is modelled by assuming the appropriate boundary condition on one of the walls restricting the flow region. The potentials to reduce methane hazards by the use of free jet fans are explored. The fan WLE-603B is installed in the inlet cross-section of the niche (x=5 m), in three positions:

a) half-way the section width, 0.5 m from the roof
b) in the upper corner of the inlet cross-section
c) in the lower corner of the inlet cross-section, and
d) underneath the roof, at the distance x =4 m from the niche front
e) underneath the roof, at the distance x=6 from the niche front

Fig 5-6 and 7-8 show velocity fields and distributions of mass fractions of methane at selected cross-sections. The most favourable variants are those designated as b (Fig 5, 7) and c and e, where the fan is positioned in the upper or lower corner of the inlet cross-section or when it is pushed into the through-flow stream. Registered differences between these solutions are minor and prove to be negligible in practical applications.

Introduction

CFD models are widely used to solve most complex problems involving the transport of mass, momentum and energy. They are widely employed in industrial applications and recently also in mine ventilation projects. 3D numerical simulations allow the major ventilation parameters to be determined: flow velocity, air temperature and concentration of gaseous components, which affords us the means to assess the efficiency of the ventilation system and to identify potentially hazardous zones. Test data reveal that most CFD models capture the flow parameters with sufficient precision for practical purposes.

The presence of methane is a major natural hazard encountered in underground coal mines. The longwall districts are often ventilated using a U- tube

ventilation, hence the potentially hazardous zones where the methane concentrations would be highest are longwall crossings with return airways. In order to reduce this hazard, auxiliary ventilation equipment (jet fans, brattices, jet exhausters) are installed in the outlet sections. The effectiveness of the employed solution might be evaluated by numerical simulations. In further chapters we analyse how the positions of jet fans, installed at the outlet from the longwall region, should affect the efficiency of methane rarefaction and removal from the area. The calculation procedure utilises the program FLUENT 6.1.

Flow region

The flow region comprising two intersecting galleries (end section of the longwall with the return) is shown in **Fig 1**. The major simplification is that the gallery walls are regarded as impermeable to mass. Methane inflow from the rock strata is modelled by assuming an appropriate boundary condition on one of the inlets (**Fig 1**). Galleries' cross-sections are taken as squares with the sides 2.5 m, the length of the blind gallery (a niche) is 5 m, the length of the inlet section (longwall end section) – 6 m and the outlet section (return) – 30 m. The latter is associated with the form of the boundary condition at the outlet- there is a fully developed velocity profile in the outlet cross-section.

Mathematical model

The air-methane mixture is assumed to be an ideal and compressible gas and hence the Clapeyron formula is applicable. The motion of this mixture is steady and process conditions are taken as isothermal. Selection of an appropriate CFD model is a major consideration and presents certain difficulties. Most authors who solved purely engineering problems would tend to choose models based on Reynold's averaging hypothesis, preferring for those utilising Boussinesq's hypothesis. In his doctor dissertation, S. Silverster analysed the current expertise in the field of mine ventilation using CFD methods, which led him to the conclusion that a standard k-ε model (kinetic energy turbulence – energy dissipation rate) seems most favourable as it best emulates the real flow parameters. This model is in widespread use in industrial applications and is widely reported in literature: [Konduri et al., 1997], [Lipska 1997], [Wala et al. 2001], [Silvester 2002], [Branny 2003], [Young 2004].

Air is assumed to be a mixture of three components: nitrogen, oxygen and water vapour. The local density of this gaseous mixture is given by the formula:

$$\rho = \frac{p}{R\,T \sum_i \frac{Y_i}{M_i}} \qquad \text{…..(1)}$$

where: p – pressure, Pa

R- universal gas constant, J/mol K

Y_i - mass fraction of the i-th component of gas mixture,

M_i- molar mass of the i-th component of gas mixture, kg /mol

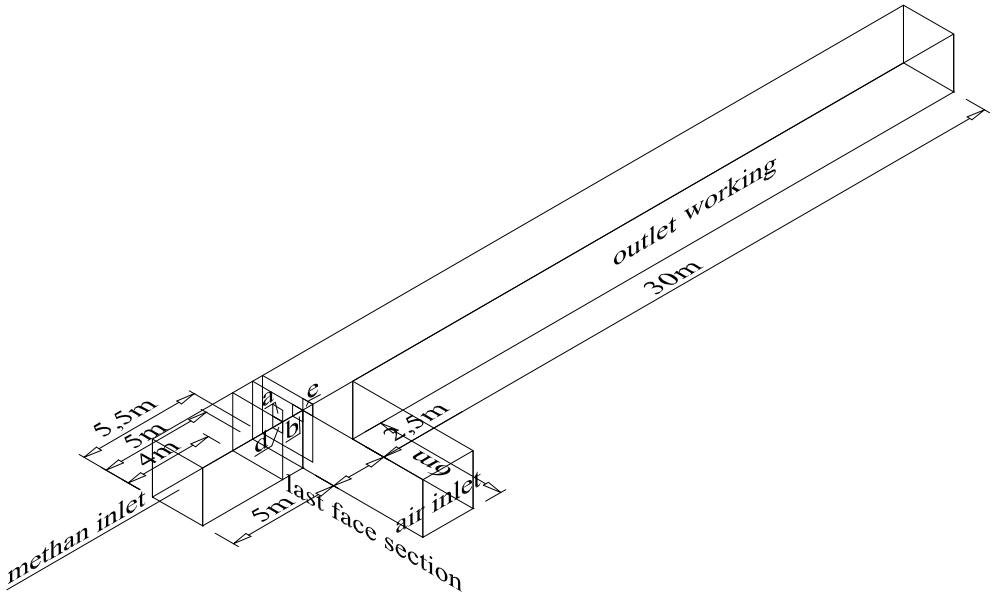

Fig. 1 Dimensions of flow region

In the FLUENT program the local mass fraction of the i-th component is obtained by solving a transport equation. The investigated problem is governed by the system of equations of continuity (2), Navier-Stokes equations, the turbulent viscosity k-ε model and the general model of transport of chemical components (3) [FLUENT Inc 2005], [Kazimierski 2004].

$$\frac{\partial(\rho v_j)}{\partial x_j} = 0 \qquad \text{…..(2)}$$

$$\frac{\partial}{\partial x_j}(\rho v_j \phi) - \frac{\partial}{\partial x_j}(\Gamma \frac{\partial \phi}{\partial x_j}) = S_\phi \qquad \text{…..(3)}$$

The interpretations of the variable Φ, the coefficient Γ and the source term S_Φ are given in **Table 1**.

Table 1. Interpretation of terms present in equation (3)

Φ	Γ	S_Φ
v_i	μ_{ef}	$\frac{\partial}{\partial x_j}(\mu_{ef}\frac{\partial v_j}{\partial x_i}) - \frac{2}{3}\frac{\partial}{\partial x_i}(\mu\frac{\partial v_l}{\partial x_l}) - \frac{\partial}{\partial x_i}(p + \frac{2}{3}k\rho\delta_{ij}) + \rho g_i$
k	$\mu + \frac{\mu_T}{\sigma_k}$	$G_k + G_b - \rho\varepsilon + V_M$
ε	$\mu + \frac{\mu_T}{\sigma_\varepsilon}$	$C_1\frac{\varepsilon}{k}(G_k + C_3 G_b) - C_2\rho\frac{\varepsilon^2}{k}$
Y_k	$\rho D_k + \frac{\mu_T}{Sc_T}$	0

Where : v_i- averaged velocity vector's component in the i-th direction, m/s

ρ- local density of the medium, kg/m^3

$\mu_{ef} = \mu + \mu_T$ – molecular and turbulent viscosity coefficient, respectively, kg/m s

g_i- gravity acceleration vector component in the i-th direction, m^2/s

k- kinetic energy of turbulence, m^2/s^2

ε- dissipation rate of kinetic energy of turbulence, m^2/s^3

D_k- kinetic coefficient of molecular diffusion of the k-th components, m^2/s

Sc_T - turbulent Schmidt number

δ_{ij}- Kronecker's symbol

C_1, C_2, C_3, σ_k, σ_ε- model constants

The terms expressing the generation of kinetic energy of turbulence due to the gradient of the (averaged) velocity field G_k, buoyancy force G_b and volumetric dissipation V_M are written as:

$$G_k = \mu_T\left(\frac{\partial v_i}{\partial x_j} + \frac{\partial v_j}{\partial x_i}\right) - \frac{2}{3}\left(\rho k + \mu_T\frac{\partial v_i}{\partial x_i}\right)\delta_{ij}$$

$$G_b = -g_i\frac{\mu_T}{\rho Pr_T}\frac{\partial \rho}{\partial x_i}$$

$$V_M = 2\rho\varepsilon M_T^2,\ \ M_T = \sqrt{\frac{k}{\rho g R T}}$$

where: Pr_T- turbulent Prandtl number

The term V_M is of minor significance in the investigated flow. It is, nevertheless, always taken account of by the FLUENT program in the case of compressible fluids.

Boundary conditions.

- Predetermined in the inlets is the constant mass flux of air and methane. Kinetic energy of turbulence and energy dissipation rate are obtained assuming 10% turbulence intensity at the inlet. Mass fractions of individual components of the gas mixture for air are: Y_{N_2} = 0.76, Y_{O_2} = 0.23, Y_{H_2O} = 0.01, and for methane: Y_{CH_4} = 1.0.
- The pressure in the inlet cross-section is taken as constant. As regards the remaining variables, it is assumed that $\frac{\partial \phi}{\partial x} = 0$ in the direction of the flow.
- The description of the boundary layer conditions utilised the classical model of the boundary wall function.

In the FLUENT program wall unevenness is modelled by predetermining the average roughness dimension.

Research conducted by Hargreave reported in [Silvester 2002] showed that satisfactory results were obtained when the roughness dimension was taken as 0.05 m and this value is taken in further calculations. It is worthwhile to mention that the widely reported wall function model available in FLUENT was developed for less rough surfaces that those encountered in mine excavations. The roughness factor is defined by the distance between the first line of nodes in the numerical grid, adjoining the rigid walls. This distance must not be less than the roughness factor as the reverse assumption is simply not feasible. The wall function is modified by incorporating the roughness term, yielding [FLUENT Inc 2005], [Hargreves, Lowndes, 2001], [Puzyrewski, Sawicki 1987]:

$$\frac{v_p v^*}{\tau/\rho} = \frac{1}{\kappa}\ln(E\frac{\rho v^* y_p}{\mu}) - \Delta B \qquad \text{.....(4)}$$

where: v_p, τ_p- velocity and tangent stress at the distance y_p from the wall

$$v^* = C_\mu^{1/4} k^{1/2}$$

E i C_μ - model constants

κ - von Karman constant

ΔB – term to account for surface roughness

The relationship (4) applies to the dimensionless quantity $\frac{\rho v^* y_p}{\mu}$ falling in the interval 30-60. In real conditions of mining excavations the upper limit might be vastly exceeded. The lack of a sufficiently well tested description of boundary conditions may become a source of inaccuracy in numerical representation of real flows [Lipska 1997], [Branny 2003].

Discretization of the flow region

The flow region is covered by the structural grid making up 240 625 elementary cells. With such grid density, the results are found to be independent of the grid size. For comparison, numerical modelling of ventilation in headings being developed utilises the grids comprising 60 000 to 150 000 elementary cells [Silvester 2002].

Analysis of results

In qualitative terms the velocity field is shown in **Fig 2**, assuming there was no auxiliary ventilation and no methane inflow to the gallery. This velocity field profile will change when methane starts flowing to the region through the front section of the niche- **Fig 3**. The buoyancy force, due to the difference in density between the two mixing media, causes a partial change of the flow direction. The air flows into the niche near the floor and leaves it flowing near the roof. The amount of air flowing through the niche is increased, too. Maximal velocities registered in the relevant cross-sections (**Fig 3** and 2), counting front the niche front are: 2.19 m/s (0.33 m/s); 1.2 m/s (0.66 m/s), 1.34 m/s (1.11 m/s). The quantities in brackets denote air velocity when no methane flows into the niche. **Fig 4** shows the distribution of mass fractions of CH_4. The cross-section- averaged and maximal values of Y_{CH_4} for the cross-sections x=0.5m, x=2.5 m and x=5.0m are: 0.1352 (0.3226); 0.1260 (0.2686); 0.0902 (0.2405). It is worthwhile to mention that for a constant air density (**Fig 2**) a 2D flow geometry would be fully justified.

The potentials to reduce methane hazards by the use of free jet fans are explored in further examples. The fan WLE-603B is installed in the inlet cross-section to the niche (x=5 m), in three positions:

a) half-way the section width, 0.5 m from the roof

b) in the upper corner of the inlet cross-section

c) in the lower corner of the inlet cross-section, and

d) underneath the roof, at the distance x =4 m from the niche front

e) underneath the roof, at the distance x=6 from the niche front

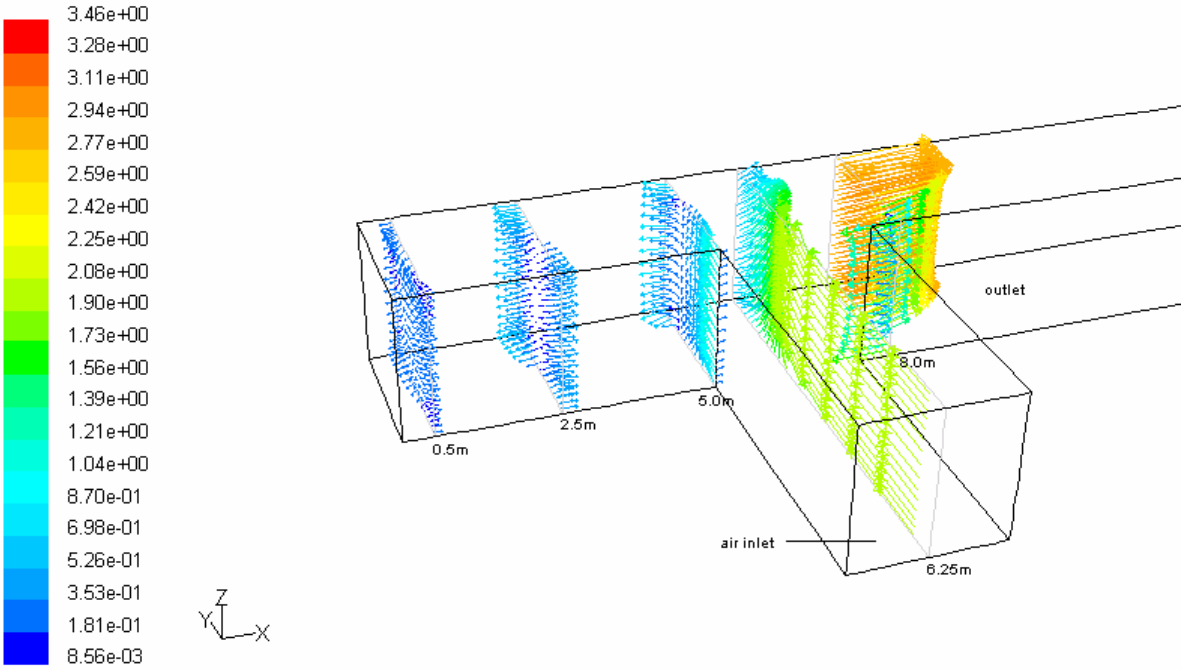

Fig. 2 Plot of velocity vectors without methane inflow from strata (constant air density)

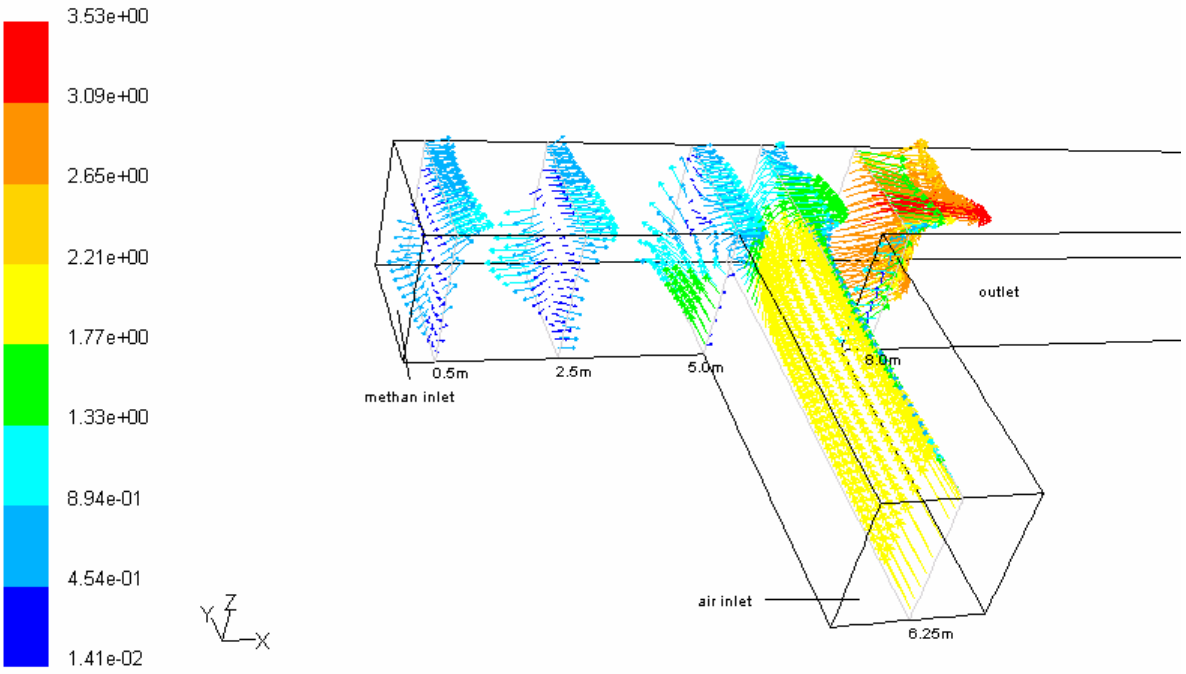

Fig. 3 Plot of velocity vectors with methane inflow from strata

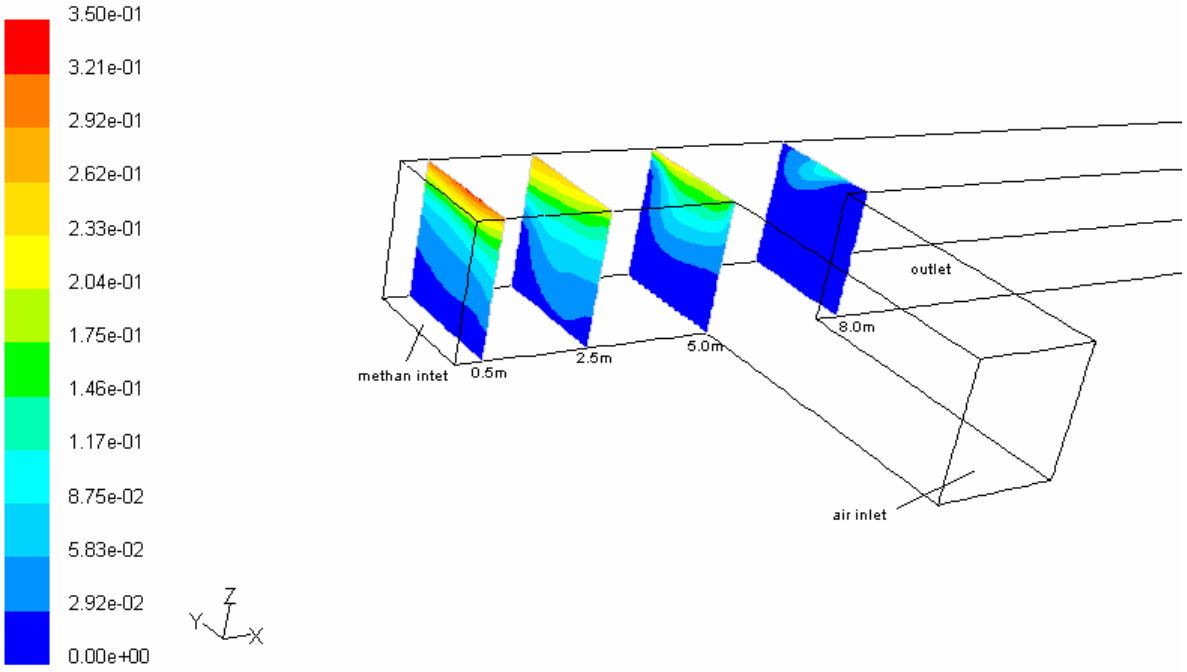

Fig. 4 Contours of mass fraction of CH_4 – inflow of methan through the front of niche

Fig 5-6 and **7-8** show some results presenting velocity fields and distributions of mass fractions of methane at selected cross-sections. The most favourable variants are those designated as b (**Fig 5, 7**) and c and e, where the fan is positioned in the upper or lower corner of the inlet cross-section or when it is pushed into the through-flow stream. Registered differences between these solutions are minor and prove to be negligible in practical applications. The highest methane concentrations are reported when the fan is located inside the niche (variant d, **Fig 6, 8**) or underneath the roof, half-way the niche width (variant a). In all considered configurations with jet fans the flow recirculation will occur. Its negative impacts are revealed when the proportion of the air-methane mixture in the recirculating stream should increase, as in the schemes a and d. Surface-averaged mass fractions of CH_4 at selected cross-sections are shown in **Fig 9**. The differences between calculated parameters of fan performance obtained for various fan positions amount to several percent. The largest registered flow rate of a fan is 8.51 kg/s (variant e), the smallest- 7.93 kg/s (variant d). The air stream generated by a fan at the distance 0.5 m from the niche front would develop the maximal velocities: 5.38 m/s (variant a) and 15-17.77 m/s for the remaining schemes. These differences might be attributable to typical behaviours of free and bounded jets despite entirely different conditions for air stream formation in the investigated space.

Numerical calculations capture also the secondary flow zone associated with the reversal of flow direction of the through-flow stream due to stream separation at the point where the longwall and the return airways should cross. The secondary flow zone is present in all considered variants, even when no jet fans are used. For the steady flow rate, the volume of the secondary flow region depends on the actual fan position. Apparent differences between the computed average mass fractions of methane (**Fig 9**) in the outlet cross-section for x=8.0 m are caused by this very phenomenon. The secondary flow zone tends to expand when a larger fan is used or when the air volume flux in the through-flow stream should decrease. For example, a 40% reduction of the amount of air in the through-flow stream brings about an increase of a cross-section-averaged mass fraction of methane by nearly 90% (Y_{CH_4} = 0.0192) at the point x=8.0 m (variant e).

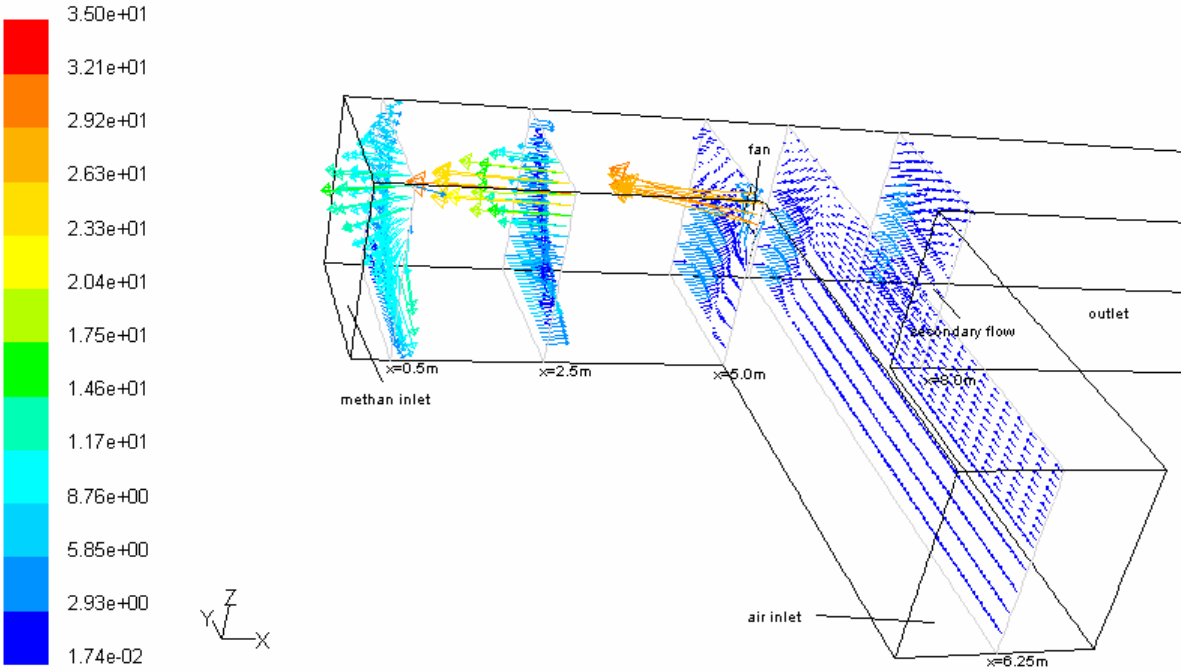

Fig. 5 Plot of velocity vectors – variant b – jet fan in the upper corner of the inlet cross-section of niche (x=5.0m)

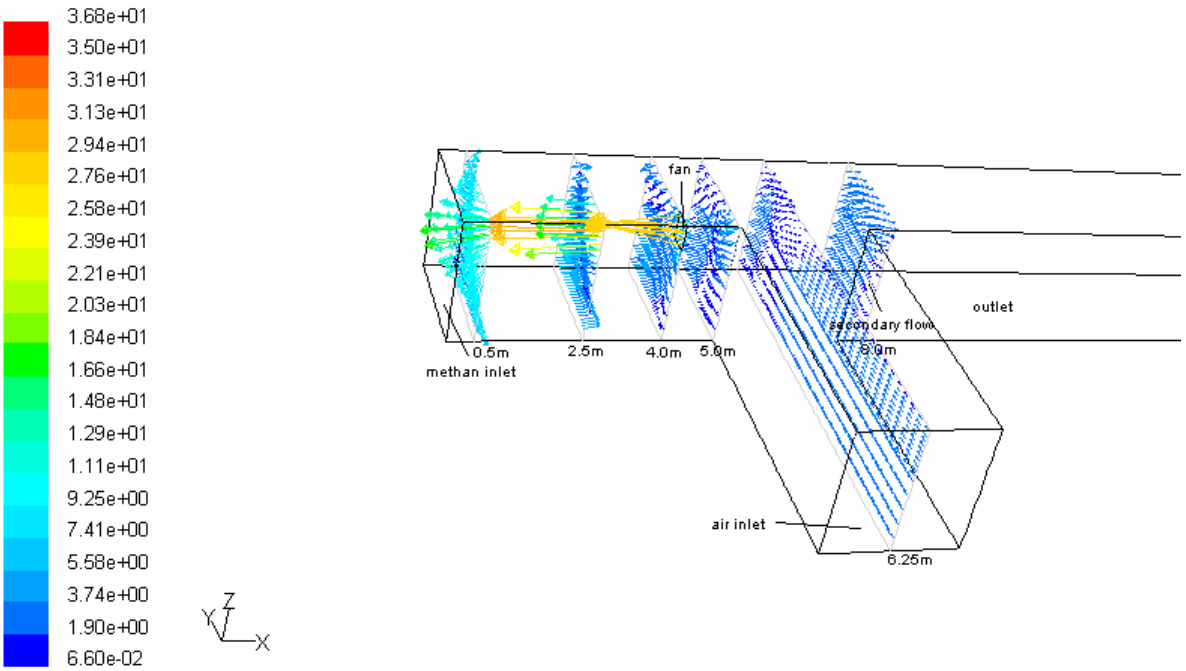

Fig. 6 Plot of velocity vectors – variant d – jet fan in the upper corner of niche at the distance x=4 m from its front

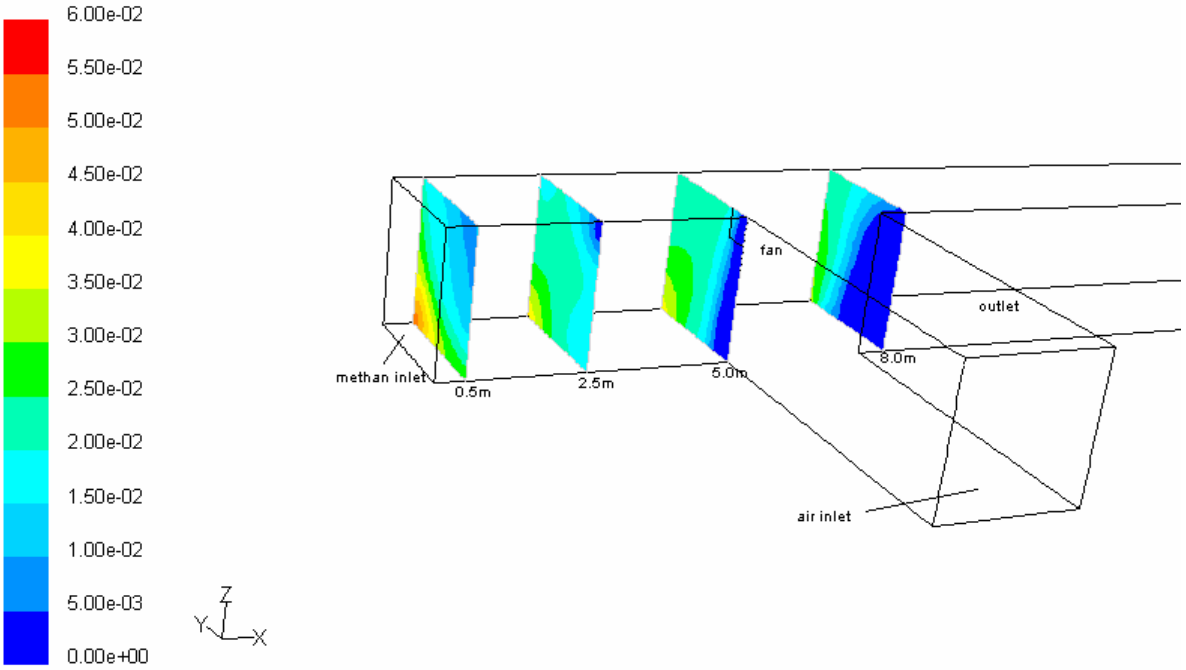

Fig. 7 Contours of mass fraction of CH_4 – fan's location as in variant b

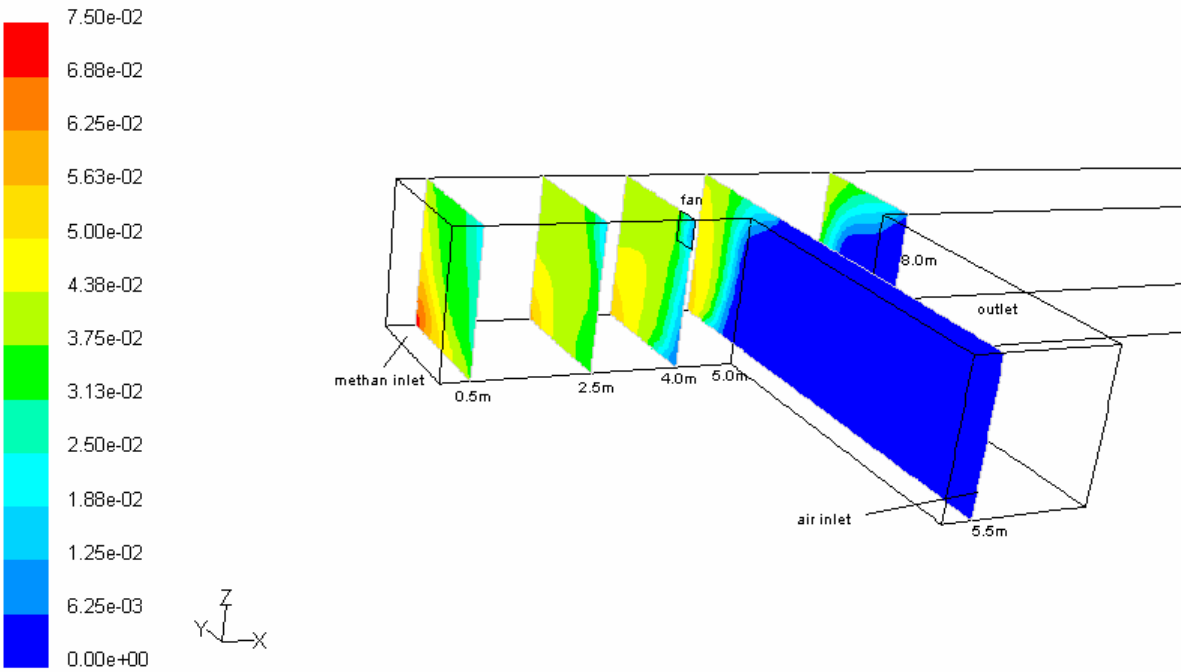

Fig. 8 Contours of mass fraction of CH_4 – fan's location as in variant d

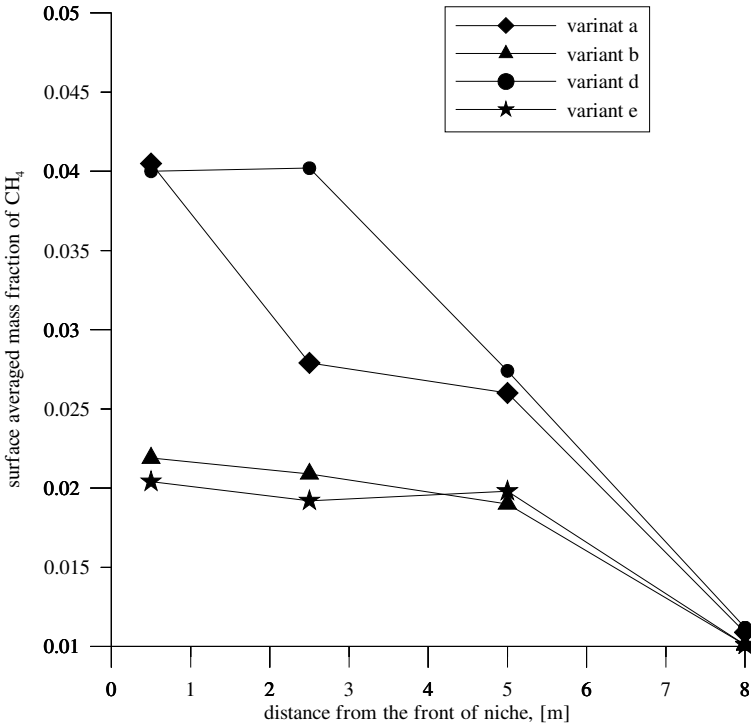

Fig. 9 Surface- averaged mass fraction of CH_4 at selected cross-sections

Conclusions

CFD models are widely applied to solve mine ventilation problems on the local scale: ventilation of longwall sections, excavations or blind galleries. Thus obtained fields of velocity, pressure, concentration of gaseous components, air temperature, humidity and dust levels become the starting point for comprehensive studies of ventilation conditions. Several reports in literature confirm the validity of CFD models in practical applications.

An jet fan employed to reduce the methane hazard in a longwall end section ought to be installed at the end of the last longwall section, near the niche (variants b,c,e). The air stream generated by the fan WLE-603B is sufficiently powerful to effectively rarefy and eliminate from the area the predetermined amount of methane coming from the rock strata. A similar study can be conducted for each individual case to be encountered in the mining practice. Account could be taken for other auxillary ventilation devices such as brattices, exhausters.

The fundamental simplification assumed in this study is that all walls are treated as impermeable to mass, that refers also to walls restricting the flow from the goaf. FLUENT program gives us the option to declare at that point a boundary separating the fluid from the solid (porous) medium. Apparently the investigated region would be extended to include the porous medium, whose physical parameters and seepage flow model would have to be specified. The goaf zone is an irregular region of rock rumble, near the longwall front there are also voids of considerable volume. A full and adequate description of fluid flow through such medium is not available, hence there are no adequate data to select a reliable model of the seepage flow. Further research in this field seems fully merited.

This study is sponsored by the Ministry of Science and IT, as a part of the research grant no 5 T12A 009 24.

References

1. Branny M.: 2003. **Numerical simulation of airflow in blind headings ventilated with jet fans**. *Archives of Mining Sciences*,48, 425-443.
2. FLUENT Inc. 2005. FLUENT 6.1 Documentation
3. Hargreves D.M., Lowndes I.S.: 2001. **An Assesment of the Future Use of Computentional Fluid Dynamics for**

Network Modeling. Proceedings of the 7th International Mine Ventilation Congress, Kraków, 547-553

4. Kazimierski Zb.: 2004. **Podstawy Mechaniki Płynów i Metod Komputerowej Symulacji Przepływów**. Politechnika Łódzka
5. Konduri I.M., McPherson M.J., Topuz E.: 1997. **Experimental and Numerical Modelling of Jet Fans for Auxiliary Ventilation in Mines**. Proceedings of the 6th International Mine Ventilation Congress, Pittsburg
6. Lipska B.: 1997. **Rezultaty badawcze ANEKSU 26 IEA w zakresie prognozowania przepływów wentylacyjnych**. Piąte Ogólnopolskie Sympozjum "Zastosowanie Mechaniki Płynów w Inżynierii Środowiska", Gliwice-Wisła, 199-213
7. Puzyrewski R., Sawicki J.: 1987. **Podstawy Mechaniki Płynów i Hydrauliki**. PWN Warszawa
8. Ren T.X., Edwards J.S., Jozefowicz R.R. 1997. **CFD Modelling of Methan Flow Around Longwall Faces**. Proceedings of the 6th International Mine Ventilation Congress. Pittsburg, 247-251
9. Silvester S.A.: 2002. **The Integration of CFD and VR Methods to Assist Auxiliary Ventilation Practice**. PhD Thesis. The University of Nottingham, Nottingham
10. Wala A.M.,Stoltz J.R., Jacob J.D. 2001. **Numerical and Experimental Study of a Mine Face Ventilation System for CFD Code Validation**. Proceedings of the 7th International Mine Ventilation Congress, Kraków, 411-418
11. Young T.: 2004. **CFD and Field Testing of a Naturally Ventilated Full-Scale Building.** PhD Thesis. University of Nottingham, Nottinghm